NIH Public Access
Author Manuscript
Mol Cell. Author manuscript; available in PMC 2014 June 12.

Published in final edited form as:
Mol Cell. 2013 December 12; 52(5): 617–628. doi:10.1016/j.molcel.2013.10.014.

A Bacterial Toxin Inhibits DNA Replication Elongation Through a Direct Interaction with the β Sliding Clamp

Christopher D. Aakre[1], **Tuyen N. Phung**[1], **David Huang**[1,2], and **Michael T. Laub**[1,2,*]

[1]Department of Biology, Massachusetts Institute of Technology, Cambridge, MA 02139

[2]Howard Hughes Medical Institute, Massachusetts Institute of Technology, Cambridge, MA 02139

SUMMARY

Toxin-antitoxin (TA) systems are ubiquitous on bacterial chromosomes, yet the mechanisms regulating their activity, and the molecular targets of toxins, remain incompletely understood. Here, we identify SocAB, a new TA system in *Caulobacter crescentus*. Unlike canonical TA systems, the toxin SocB is unstable and constitutively degraded by the protease ClpXP; this degradation requires the antitoxin, SocA, as a proteolytic adaptor. We find that the toxin, SocB, blocks replication elongation through an interaction with the sliding clamp, driving replication fork collapse. Mutations that suppress SocB toxicity map to either the hydrophobic cleft on the clamp that binds DNA polymerase III or a clamp-binding motif in SocB. Our findings suggest that SocB disrupts replication by outcompeting other clamp-binding proteins. Collectively, our results expand the diversity of mechanisms employed by TA systems to regulate toxin activity and inhibit bacterial growth, and they suggest that inhibiting clamp function may be a generalizable antibacterial strategy.

INTRODUCTION

Toxin-antitoxin (TA) systems are genetic modules that are widely present on plasmids and bacterial chromosomes, with some species encoding more than 50 TA pairs (Pandey and Gerdes, 2005). Each TA system is typically comprised of a toxin and its cognate antitoxin that are encoded together in an operon; normally, both the toxin and antitoxin are synthesized and form a stable, non-toxic complex. However, under stressful conditions, the more labile antitoxin can be degraded, freeing the stable toxin to inhibit bacterial growth (Wang et al., 2011). TA systems are implicated in a number of important cellular processes, including plasmid stability, bacterial persistence, stress responses and resistance to phage (Gerdes and Maisonneuve, 2012; Yamaguchi and Inouye, 2011).

The toxins from characterized TA systems inhibit growth by targeting a relatively limited set of critical cellular functions such as translation, DNA replication, or cell wall growth. For instance, the toxin Doc inhibits translation by phosphorylating EF-Tu (Castro-Roa et al., 2013), whereas other toxins, such as MazF, block translation by cleaving mRNAs (Zhang et

© 2013 Elsevier Inc. All rights reserved.

*correspondence: laub@mit.edu.

Publisher's Disclaimer: This is a PDF file of an unedited manuscript that has been accepted for publication. As a service to our customers we are providing this early version of the manuscript. The manuscript will undergo copyediting, typesetting, and review of the resulting proof before it is published in its final citable form. Please note that during the production process errors may be discovered which could affect the content, and all legal disclaimers that apply to the journal pertain.

Accession Numbers

The expression data for cells producing SocB-M2 has been deposited in ArrayExpress with accession number E-MEXP-3990.

NIH-PA Author Manuscript
NIH-PA Author Manuscript
NIH-PA Author Manuscript

NIH-PA Author Manuscript

NIH-PA Author Manuscript

NIH-PA Author Manuscript

al., 2003). The toxins CcdB and ParE inhibit replication by binding DNA gyrase, which is required to relieve supercoiling that occurs ahead of the replication fork (Yuan et al., 2010). Additionally, the PezT toxin blocks cell wall growth by phosphorylating peptidoglycan precursors, thereby inhibiting the initial step in peptidoglycan synthesis (Mutschler et al., 2011). Strikingly, small-molecule antibiotics inhibit cellular proliferation by targeting a very similar set of processes, including translation (aminoglycosides), DNA replication (fluoroquinolones), and cell wall growth (β-lactams) (Walsh, 2003). The recent rise in antibiotic resistance (Bush et al., 2011), and the lack of diversity of current antibiotics (Coates et al., 2011), highlight the need to identify new targets within bacteria to inhibit their proliferation. The study of bacterial toxins may help elucidate such targets for the development of novel small-molecule therapeutics.

The DNA replication machinery, or replisome, could be a prime target, but is surprisingly not targeted by any known TA systems or antibiotics in clinical use (Robinson et al., 2012). Bacterial DNA replication is catalyzed by a multi-component complex known as DNA polymerase III (Pol III). The Pol III core (subunit composition αεθ) is weakly processive on its own and can only incorporate 1–10 nucleotides per binding event (Johnson and O'Donnell, 2005). To increase its processivity, Pol III core associates with the β sliding clamp, DnaN, a ring-shaped protein that encircles DNA topologically. Binding to DnaN increases the processivity of Pol III over three orders of magnitude (Johnson and O'Donnell, 2005; Maki and Kornberg, 1988). In *E. coli*, DnaN also associates with DNA Pols I, II, IV, and V (Indiani et al., 2005); the mismatch repair proteins MutS and MutL (Lopez de Saro et al., 2006); and the replication regulator Hda (Kurz et al., 2004). The interaction of these proteins with DnaN is required for a number of processes, including translesion synthesis (Lenne-Samuel et al., 2002) and mismatch repair (Lenhart et al., 2013). These clamp-binding proteins contain variants of a short peptide motif, QL[SD]LF, that mediates binding to a conserved hydrophobic cleft on DnaN (Dalrymple et al., 2001). DnaN thus forms a central hub for DNA replication and repair in bacteria.

Here, we identify an atypical TA system in *Caulobacter crescentus*, SocAB. We find that the toxin SocB is normally unstable and constitutively degraded by the protease ClpXP. In contrast to canonical TA systems, in which the antitoxin neutralizes its toxin by sequestration, we find that the antitoxin SocA neutralizes SocB by acting as an adaptor for the degradation of SocB by ClpXP. The requirement of ClpXP for SocB degradation explains for the first time why ClpXP is essential for viability in *Caulobacter*. Additionally, we provide evidence that SocB inhibits replication elongation through a direct interaction with DnaN. Mutations in DnaN or SocB that block their association occur in the hydrophobic cleft in DnaN or in a DnaN-binding motif in SocB, suggesting that SocB binds to DnaN in a similar manner as known clamp-binding proteins and competes for binding to DnaN during replication. In sum, our work elucidates novel mechanisms employed by TA systems to regulate toxin function and to inhibit cellular proliferation. Our results further suggest that protein interaction hubs such as DnaN may be ideal targets for the development of new protein- or small-molecule-based antimicrobials.

RESULTS

Mutations in the Toxin *socB* Can Bypass the Essentiality of *clpXP*

ClpXP is a widely conserved AAA+ protease that uses the power of ATP hydrolysis to unfold and proteolyze substrates within cells (Sauer and Baker, 2011). ClpXP is comprised of two proteins: the unfoldase ClpX, which recognizes and unfolds substrates, and the peptidase ClpP, which degrades the unfolded substrates that it receives from ClpX. Unlike most bacteria, *clpX* and *clpP* are essential for viability in *Caulobacter* (Jenal and Fuchs, 1998). To identify factors responsible for *clpP* essentiality, we selected for transposon

NIH-PA Author Manuscript

NIH-PA Author Manuscript

NIH-PA Author Manuscript

insertions that allow cells to grow in the absence of *clpP* expression. We identified multiple transposon insertions in a hypothetical gene (CCNA_03629) that we named *socB* for suppressor *o*f *clpXP* (Fig. 1A). A clean deletion of *socB* allowed cells to grow in the absence of either *clpX* or *clpP* expression (Fig. 1B); however, growth was slower on medium that repressed *clpX* or *clpP*, consistent with the fact that ClpXP degrades a range of cellular proteins (Bhat et al., 2013).

To better assess the ability of *socB* mutants to suppress *clpX* essentiality, we used a *clpX* depletion strain and performed a time-course experiment following the switch to non-inducing medium. Using immunoblotting, we found that ClpX gradually declined to almost undetectable levels after 10 hours (Fig. 1C) (Jenal and Fuchs, 1998). In $socB^+$ cells, the depletion of ClpX coincided with an increase in cellular filamentation (Fig. 1D) and a more than 1000-fold decrease in colony-forming units (CFUs) (Fig. 1E). However, in cells lacking *socB*, we observed only intermediate filamentation and no drop in CFUs (Fig. 1D–E). These data support the conclusion that a *socB* deletion bypasses the essentiality of *clpXP*.

socB is present in an operon with an upstream gene, *socA*, that is predicted to be essential (Fig. 1A) (Christen et al., 2011). This observation raised the possibility that *socAB* may encode a TA system. To test this hypothesis, we placed the putative toxin *socB* under an inducible promoter and tested whether its expression was toxic to cells in the presence or absence of its putative antitoxin *socA*. We found that inducing *socB* in *socA*+ cells had no significant effect on cell viability or morphology (Fig. 1F–G). However, inducing *socB* in Δ*socA* cells inhibited colony formation and led to cellular filamentation (Fig. 1F–G). These phenotypes could be rescued by expressing *socA* in *trans* from a plasmid behind a different inducible promoter. Furthermore, time-course experiments revealed an approximately 10-fold decrease in viability in cells expressing *socB* for 5 hours in the absence of *socA* (Fig. S1A–B). Collectively, our data indicate that *socAB* behaves genetically like other TA systems.

For type II TA systems, the antitoxin functions by forming a complex with its cognate toxin and neutralizing its activity (Yamaguchi et al., 2011). To test whether SocA and SocB directly interact, we used the bacterial two-hybrid system based on complementation of the T18 and T25 fragments of adenylate cyclase (Karimova et al., 1998). We fused *socA* and *socB* to the T25 and T18 fragments, respectively, and co-expressed the gene fusions in *E. coli*. We observed a strong interaction between SocA and SocB, indicating that they likely form a complex (Fig. 1H). Interestingly, *socB* expression did not kill *E. coli*, indicating that its toxicity may be phylogenetically restricted. Indeed, homologs of *socAB* were identified only in the α-proteobacteria (Fig. S1C).

SocA Promotes SocB Degradation by ClpXP

The observation that a deletion of *socB* can bypass the essentiality of ClpXP suggested that SocB may be a ClpXP substrate, and that accumulation of SocB in the absence of ClpXP inhibits growth. To test this possibility, we measured the accumulation of an M2-tagged variant of SocB in the presence or absence of ClpX. Whereas no M2-SocB was detected in the presence of ClpX, M2-SocB accumulation was observed when ClpX was first depleted for 12 hours (Fig. 2A). To confirm that the decreased abundance of SocB in the presence of ClpX results from a change in protein stability, we produced M2-SocB from a plasmid and measured its half-life in the presence or absence of ClpX using a chloramphenicol shut-off assay. We found that the presence of ClpX reduced the half-life of M2-SocB from >60 min to ~15 min, indicating that SocB is likely a ClpXP substrate (Fig. 2B, S2A).

Based on these results, we reasoned that SocB is normally present at low levels due to constitutive degradation by ClpXP. What role, then, does SocA play in the neutralization of

NIH-PA Author Manuscript

NIH-PA Author Manuscript

NIH-PA Author Manuscript

SocB? Antitoxins of TA systems typically neutralize their cognate toxins by forming a stable complex (Yamaguchi et al., 2011). However, given that SocB is normally unstable, SocA may instead neutralize SocB by promoting its degradation. Indeed, we observed that M2-SocB accumulated in a strain lacking *socA*, but not in a *socA*+ strain (Fig. 2C). To test whether SocA affects the stability of SocB, we measured the half-life of M2-SocB with and without *socA* expression from a low-copy plasmid. We found that SocA reduced the half-life of M2-SocB from ~19 to ~2 min, indicating that SocA promotes the degradation of SocB (Fig. 2D, S2B). The half-life of M2-SocB in the presence of SocA (~2 min) was shorter than that measured above (~15 min), presumably due to differences in *socA* expression from a low-copy plasmid compared to its native chromosomal locus.

We hypothesized that SocA may be an adaptor for SocB degradation by ClpXP. Canonical adaptors, such as SspB, tether their substrates to the N-domain of ClpX. This tethering increases substrate concentration around the ClpX pore, which concomitantly increases the rate of substrate degradation (Dougan et al., 2003; Levchenko et al., 2000). To test whether SocA is a proteolytic adaptor, we purified SocA and SocB and performed an *in vitro* degradation reaction with ClpXP. When SocB was combined with ClpXP alone, no degradation was observed (Fig. 2E). However, when an equimolar amount of SocA was added to the reaction, we observed robust degradation of SocB, indicating that SocA promotes the degradation of SocB by ClpXP (Fig. 2E).

We performed the same reaction with a variant of ClpX that lacks the N-domain (residues 1–62) and, consequently, is catalytically active but deficient in adaptor-mediated degradation (Dougan et al., 2003). We observed no detectable degradation of SocB in the presence of SocA, ΔN-ClpX, and ClpP, indicating that the N-domain of ClpX is required for SocA to promote SocB proteolysis (Fig. 2E). Further, we observed a direct interaction between the ClpX N-domain and SocA (Fig. S2C), and found that mutations in the ClpX N-domain that abolish the interaction between ClpX and SocA prevent SocA from functioning as an antitoxin *in vivo* (Fig. S2D). Collectively, these data indicate that SocA is an adaptor for the degradation of SocB by ClpXP and they explain why *clpXP* and *socA* are essential for viability in *Caulobacter*.

Accumulation of SocB Blocks Replication Elongation

Why is the accumulation of SocB toxic to *Caulobacter* cells? To better study SocB function, we sought to develop a stabilized variant that is toxic even in the presence of SocA and ClpXP. Because ClpX often recognizes the free C-terminus of its substrates (Flynn et al., 2003), we tested the effect of appending an M2 tag to SocB. We found that SocB-M2 was stabilized over 40-fold relative to M2-SocB (Fig. S3A) and was toxic to *socA*+ *clpXP*+ cells (Fig. S3B). This stabilized variant was subsequently used to assess the effects of SocB on cellular physiology.

Toxins of TA systems target a diverse range of targets within bacterial cells (Yamaguchi et al., 2011). Two observations suggested that SocB inhibits DNA replication at the level of elongation. First, induction of *socB-M2* caused cellular filamentation without chromosome accumulation, which may indicate that growth continues while replication elongation is blocked (Fig. S3C). Second, global expression profiling indicated that *socB-M2* expression induced the SOS response (Fig. 3A). The SOS response is often induced in response to replication perturbations, such as DNA damage, that disrupt replication fork progression (Little and Mount, 1982). To directly test whether replication elongation is inhibited by SocB, we measured DNA content in synchronized populations of cells harboring an inducible copy of *socB-M2*. In non-inducing conditions, DNA content increased linearly as a function of time post-synchrony (Fig. 3B). In contrast, the induction of *socB-M2* caused a decrease in the rate of replication elongation, and cells eventually arrested with a DNA

NIH-PA Author Manuscript

NIH-PA Author Manuscript

NIH-PA Author Manuscript

content between 1N and 2N (Fig. 3B). As the completion of DNA replication is required for cell division, these cells also failed to divide (data not shown). These results indicate that SocB inhibits replication primarily at the level of elongation.

SocB Blocks Replication Through an Interaction with DnaN

To identify the putative target of SocB, we screened for mutants that can tolerate high levels of *socB-M2* expression. The first suppressors recovered were mutations in *clpX* that destabilized SocB-M2 (Fig. S3D). The largest group of these mutations clustered near the RKH loop, which protrudes from the ClpX pore and is important for the recognition of SsrA-tagged substrates (Farrell et al., 2007; Martin et al., 2008). Additional mutations were found at sites distant from the ClpX pore: Y76 and P326, for example, are proximal to the ATP-binding site and roughly 40 Å away from the nearest RKH loop. In each tested case, the mutations resulted in an approximate 10-fold reduction in SocB-M2 stability (Fig. S3E).

To identify suppressors outside of *clpX*, we continued our screen but focused on isolates that retained high levels of SocB-M2 and that did not harbor mutations in *clpX*. For two mutants, whole-genome sequencing revealed point mutations in *dnaN*, which encodes the β sliding clamp required for the processivity of DNA replication (Johnson and O'Donnell, 2005). Both mutations led to substitutions in glycine-179 of DnaN: G179C and G179R. We introduced these *dnaN* mutations into a clean genetic background and found that each was sufficient to bypass the replication block and growth inhibition normally observed following *socB-M2* expression (Fig. 3C–D). Furthermore, these mutations were able to partially suppress the filamentation observed following SocB-M2 accumulation (Fig. S3F).

Glycine-179 resides within the hydrophobic groove on DnaN that is required for binding to Pol III and other replication proteins (Fig. 3E) (Georgescu et al., 2008). The identification of suppressor mutations affecting this residue of DnaN raised the possibility that SocB blocks replication through a direct interaction with DnaN. To test this possibility, we purified SocB-GST and DnaN and measured their binding by affinity chromatography *in vitro*. Production of SocB-GST is toxic to *Caulobacter*, indicating that this fusion protein is functional (Fig. S3G). We observed a strong interaction between DnaN and SocB-GST, but no interaction when DnaN was incubated with GST alone (Fig. 3F). Importantly, the suppressor mutations in DnaN, G179C and G179R, each disrupted the interaction with SocB-GST (Fig. 3F). We obtained similar results using a bacterial two-hybrid system, confirming that DnaN and SocB can directly interact (Fig. S3H).

The suppressor mutations isolated in DnaN reside within a hydrophobic groove required for its interaction with DnaN-binding proteins such as HdaA (Jonas et al., 2011), which must bind DnaA to regulate replication initiation (Kato and Katayama, 2001). To determine whether these mutations disrupt the interaction of DnaN with HdaA, we repeated our interaction assay and found that DnaN(G179C) retained the ability to interact with HdaA, whereas the G179R mutant did not (Fig. S3H). Consistent with these binding data, cells producing DnaN(G179C) appeared similar to wild type in the absence of *socB* expression, suggesting that the mutant version of DnaN supported wild-type like growth. In contrast, cells producing DnaN(G179R) were often filamentous (Fig. S3F), indicating that the interaction between DnaN and other proteins such as HdaA may be compromised. Taken together, our results support a model in which SocB blocks replication elongation through an interaction with DnaN, and that mutations in the hydrophobic cleft on DnaN can abrogate binding of SocB.

NIH-PA Author Manuscript

NIH-PA Author Manuscript

NIH-PA Author Manuscript

SocB Induces Loss of DnaN Replication Foci and Replication Fork Collapse

During DNA replication, DnaN accumulates dynamically behind the lagging strand polymerase as a result of discontinuous DNA replication; consequently, YFP-tagged DnaN typically forms a discrete focus within cells during replication (Su'etsugu and Errington, 2011). Additionally, in *Caulobacter*, DnaN translocates along the major axis of the cell during replication (Collier and Shapiro, 2009). To determine whether DnaN dynamics (and by proxy, ongoing replication) are affected by SocB, we imaged YFP-tagged DnaN in a strain harboring an inducible copy of *socB-M2*. In the absence of *socB-M2* expression, G1-phased cells typically showed diffuse DnaN-YFP followed by formation of a single focus after the initiation of DNA replication (Fig. 4A). The focus moved along the major axis of the cell until its dispersal at the end of replication (Fig. 4B). In the presence of *socB-M2* expression, we also observed formation of a single DnaN-YFP focus following initiation, but the focus often dispersed much earlier (Fig. 4C–D). In cells that lost their DnaN-YFP focus earlier, transient focus formation was sometimes observed following initial focus loss (Fig. 4C–D) although these foci often lasted only a single frame and appeared at varying points along the cell axis.

To quantify these effects, we measured the time from focus formation to dispersal (τ_{focus}), which reflects how long Pol III is engaged in replication before disengaging (either as a result of replication completion or pre-mature termination). We found that the average focus duration, τ_{focus}, dropped from 89 to 61 minutes in the presence of *socB-M2* expression (Fig. 4E, $p<10^{-8}$). Multiple observations indicated that the decrease in τ_{focus} represented fork collapse prior to the completion of replication. First, measurements of τ_{focus} in the absence of *socB-M2* expression indicated that replication takes, on average, 89 minutes to complete, and that no cells finish prior to 40 minutes post initiation (Fig. 4F); in the presence of *socB-M2* expression, however, 34% of cells terminated replication prior to 40 minutes, indicating that these cells most likely suffered collapsed forks and harbored incompletely replicated chromosomes. Second, measurements of DNA content in the DnaN-YFP strain expressing *socB-M2* indicated that these cells arrest with DNA content between 1N and 2N (data not shown). Third, transient DnaN-YFP focus formation following initial dispersal is suggestive of abortive attempts at replication re-start. These findings, in addition to the observed induction of the SOS response upon expression *of socB-M2* (Fig. 3A), are consistent with a model in which SocB induces replication fork collapse.

To test whether the mutations identified in *dnaN* bypass replication fork collapse, we imaged strains expressing *dnaN(G179C)-YFP* in the presence or absence of *socB-M2* expression and calculated τ_{focus}. In contrast to cells expressing *dnaN-YFP*, we no longer observed a significant difference in τ_{focus} following the production of SocB ($p = 0.09$) (Fig. 4E,G). Whereas 34% of *dnaN-YFP* cells expressing *socB-M2* lost their foci within 40 minutes of replication initiation, only 1% of *dnaN(G179C)-YFP* cells did. These results indicate that mutations in DnaN that block binding to SocB also prevent replication fork collapse, further supporting the conclusion that SocB inhibits replication elongation through a direct interaction with DnaN.

SocB Co-Localizes with DnaN in a Replication-Dependent Manner

The interaction between SocB and DnaN suggested that SocB may localize to the replisome. To examine the subcellular localization of SocB, we integrated an inducible *socB-YFP* fusion on the chromosome and imaged cells by fluorescence microscopy. Expression of *socB-YFP* inhibited colony formation, indicating that this translational fusion is functional (Fig. S4A). After inducing *socB-YFP* for three hours, we observed the formation of SocB-YFP foci in a majority of cells (Fig. 5A). The formation of these foci was dependent on the ability of SocB to bind DnaN, as foci were rarely seen in cells producing DnaN(G179C) or

NIH-PA Author Manuscript

NIH-PA Author Manuscript

NIH-PA Author Manuscript

DnaN(G179R) (Fig. 5A). SocB foci were also dependent on ongoing replication, as we saw a significant decrease in foci formation in cells depleted of DnaA, the replication initiator protein (Fig. 5B).

To test whether SocB and DnaN co-localize during replication, we fused *dnaN* to *mCherry* at the native chromosomal *dnaN* locus. We then integrated an inducible copy of *socB-YFP* on the chromosome and imaged cells by fluorescence microscopy at hour-long intervals post *socB-YFP* induction. Using an automated image analysis pipeline (Fig. S4B–C and Extended Experimental Procedures), we calculated the percentage of cells that have DnaN-mCherry foci, and of these cells, the percentage that also have co-localized SocB-YFP foci. As expected, we observed a decrease in the percentage of cells with DnaN-mCherry foci as a function of time post *socB-YFP* induction (Fig. 5C, $p=3 \times 10^{-4}$). The percentage of cells with DnaN-mCherry foci did not decrease to zero, presumably due to cells attempting to re-start replication following initial fork collapse (Fig. 4C). Although the percentage of cells with DnaN-mCherry foci decreased over time, the percentage of cells with co-localized DnaN-mCherry and SocB-YFP increased significantly (Fig. 5C). Most co-localization-positive cells had co-localized foci at a single point along the cell axis (Fig. 5D). In a minority of cells, multiple co-localized foci could be observed, which may occur when the left- and right-arm replisomes are no longer overlapping (Fig. 5E).

To test whether these localization effects were dependent on a direct interaction between SocB and DnaN, we repeated these microscopy experiments in a strain with *dnaN(G179C)-mCherry* integrated at its native chromosomal locus. In contrast to the *dnaN-mCherry* strain, we observed no significant decrease in the percentage of cells with DnaN(G179C)-mCherry foci as a function of time post *socB-YFP* induction (Fig. 5C, p=0.23). Further, fewer than 0.3% of cells exhibited co-localization between DnaN(G179C)-mCherry and SocB-YFP at any of the measured time points, in contrast to the 24% of cells that exhibit co-localization between DnaN-mCherry and SocB-YFP at three hours post induction (Fig. 5C). These results are consistent with a model in which SocB forms foci through its association with DnaN during active replication.

SocB Interacts with DnaN Through a DnaN-Binding Motif

In γ-proteobacteria, DnaN-binding proteins such as Hda and DnaE often contain a shared motif (QL[SD]LF) for binding the β-sliding clamp. Examination of HdaA (the *Caulobacter* ortholog of Hda) and DnaE orthologs from α-proteobacteria revealed a similar, putative DnaN binding motif (Fig. 6A). SocB contained a short region similar to the DnaN-binding motif found in HdaA orthologs (Fig. 6B). To test whether this region is required for the interaction of SocB with DnaN, we generated a Q52A mutant of *socB-YFP*. Mutation of this conserved glutamine in HdaA is sufficient to abolish its interaction with DnaN (Jonas et al., 2011). We found that this mutation abolished the toxicity of *socB-YFP* expression (Fig. 6C), the formation of SocB-YFP foci (Fig. 6D), and also the interaction between SocB and DnaN (Fig. 6E, S5). Importantly, this mutation did not affect the ability of SocB to interact with SocA, indicating that SocB(Q52A) is likely properly folded (Fig. S5). These results support a model in which SocB inhibits replication by binding to DnaN using a motif similar to that of HdaA.

DISCUSSION

Essentiality of ClpXP and SocA Mechanism of Action

Unlike most bacteria, ClpXP is essential for the viability of *Caulobacter* cells (Jenal and Fuchs, 1998); however, the reason for this essentiality was not clear until now. Our work reveals that ClpXP is required for the degradation of a toxin, SocB, that is constitutively

NIH-PA Author Manuscript

NIH-PA Author Manuscript

NIH-PA Author Manuscript

produced in cells (Fig. 7, left). In the absence of ClpXP or SocA, SocB accumulates, leading to the collapse of replication forks, induction of the SOS response, and eventual cell death (Fig. 7, right). Consequently, mutations in *socB* can bypass the essentiality of *clpX* or *clpP* (Fig. 1B). We note, however, that cells lacking *socB* and either *clpX* or *clpP* do not grow as rapidly as wild-type, likely due to defects in the turnover of other ClpXP substrates such as the cell cycle regulator CtrA (Bhat et al., 2013).

The rapid turnover of SocB is unusual, given that, for most TA systems, the toxin is more stable than its cognate antitoxin. The reduced stability of SocB stems from the atypical mechanism of its antitoxin, SocA. Whereas most antitoxins inhibit their cognate toxins through sequestration, SocA is instead an adaptor for the degradation of SocB by ClpXP. SocA binds both SocB (Fig. 1H) and the N-domain of ClpX (Fig. S2C) and thereby promotes the degradation of SocB *in vivo* and *in vitro* (Fig. 2D–E). SocA binding to the N-domain appears to be essential for this activity, as SocA was unable to promote SocB proteolysis when the N-domain was truncated from ClpX (Fig. 2E). The observation that SocA decreases SocB stability does not rule out that SocA also blocks SocB toxicity through sequestration. However, multiple results argue against this role for SocA: (1) targeted mutations in the N-domain of ClpX that abolish SocA binding also prevent SocA from functioning as an antitoxin *in vivo* (Fig. S2C–D); and (2) production of the stable SocB-M2 variant in *socA*+ cells is lethal, even though SocB-M2 and SocA can still form a complex (Fig. S3B, data not shown). Thus, we propose that the antitoxin activity of SocA results principally from its ability to promote SocB proteolysis through ClpXP, which makes SocA necessary, but not sufficient, for counteracting SocB toxicity.

In many bacteria, ClpXP is not formally essential for viability, although it is often required for other critical processes. In *E. coli*, deletions of *clpX* or *clpP* have no significant effect on viability or growth rate (Schweder et al., 1996), but ClpXP contributes to the proteolysis of a range of cellular substrates (Flynn et al., 2003). In *B. subtilis*, *clpX* and *clpP* deletions are viable but have major defects in sporulation and competence (Nakano et al., 2001). These defects are mostly due to accumulation of a transcriptional regulator, Spx, that is normally degraded by ClpXP. ClpX or ClpP has, however, been found to be essential in several bacteria, including the pathogens *Mycobacterium tuberculosis* and *Streptococcus pneumoniae* (Piotrowski et al., 2009; Raju et al., 2012). The essentiality of *clpX* can be bypassed in *Streptococcus* by mutations in an uncharacterized gene, *spr1630*, suggesting that this gene product may accumulate in the absence of ClpXP and inhibit growth, similar to SocB. Characterization of the gene products that bypass ClpXP essentiality may reveal novel regulators of cell growth or physiology.

Mechanism of SocB Inhibition of Replication Elongation

Our results indicate that, upon accumulating, SocB blocks replication elongation and triggers an SOS response (Fig. 3). Multiple observations suggest that SocB mediates these effects through a direct interaction with DnaN: (1) SocB and DnaN interact *in vitro* and in a bacterial two-hybrid assay (Fig. 3F, S3H); (2) mutations in DnaN that abolish its interaction with SocB also bypass the SocB-induced replication block (Fig. 3C,F, S3H); (3) SocB and DnaN co-localize, and this co-localization is dependent on the ability of SocB and DnaN to interact (Fig. 5); and (4) SocB contains a DnaN-binding motif that is required for its interaction with DnaN and toxicity (Fig. 6). In sum, these results are consistent with a model in which SocB binds to DnaN, and that this association leads to catastrophic replication fork collapse (Fig. 4).

How, then, does the interaction between SocB and DnaN lead to the premature termination of replication? The simplest model is that SocB competes with Pol III for binding to DnaN, potentially disrupting both lagging and leading strand synthesis. During lagging strand

NIH-PA Author Manuscript

NIH-PA Author Manuscript

NIH-PA Author Manuscript

replication, the polymerase extends discontinuously and presumably must associate with a new clamp to produce each Okazaki fragment (Johnson and O'Donnell, 2005). Disruption of the Pol III-DnaN interaction could rapidly inhibit production of new Okazaki fragments and consequently block synthesis of the lagging strand. In contrast, during leading strand replication, the polymerase can extend continuously and may not need to load new clamps following initiation. However, depending on the stability of the Pol III-DnaN interaction, SocB may still be able to compete for binding to DnaN on the leading strand if Pol III and DnaN ever transiently dissociate, such as upon encountering a DNA lesion. Additionally, blocking synthesis on the lagging strand would also indirectly inhibit synthesis on the leading strand, given that the leading and lagging strand polymerases are physically tethered by the γ clamp loader complex. Such stalling of replication could eventually lead the replisome to disassemble.

Notably, the effects of SocB on DNA replication are not immediate; replication first slows down approximately 120 min post-induction (Fig. 3B, note the 90 min pre-induction prior to time zero). This timing coincides with the first observable decrease in viability (Fig. S1B) and an increase in the co-localization of SocB with DnaN (Fig. 5C), but is later than may be expected if SocB immediately outcompetes Pol III for binding to DnaN. The delay may simply reflect a need for SocB to accumulate to sufficient levels before outcompeting Pol III and other DnaN-binding proteins. Alternatively, SocB may only disrupt new associations of DnaN and Pol III such that replication can initially continue following the accumulation of SocB by using DnaN molecules already in association with Pol III.

An additional question is why SocB, despite the presence of a DnaN-binding motif, is not toxic to *E. coli* which has a similar hydrophobic pocket on DnaN (Fig. 1H, data not shown). It is possible that that SocB makes contacts with DnaN at a secondary site that is less well conserved between bacteria. Interestingly, a co-crystal structure of DnaN and the little finger domain of DNA Pol IV, a DnaN-interacting protein, revealed the presence of a secondary binding interface outside of the hydrophobic pocket (Bunting et al., 2003). The secondary interface comprised over 70 percent of the buried surface area, indicating that it likely contributes significantly to the affinity of interaction. The requirement of a secondary binding interface may explain why appending a DnaN-binding motif to GFP only results in weak DnaN-dependent foci formation in *B. subtilis* (Su'etsugu and Errington, 2011).

Given the ability of SocB to inhibit replication progression, an important remaining question is when SocB normally accumulates in wild-type cells. Genetically, we revealed that a loss of *clpX*, *clpP*, or *socA* is sufficient to allow SocB accumulation (Fig. 1B, 2). Whether the stability or activity of ClpXP, or SocA, is ever modulated to induce SocB accumulation is not yet clear. Intriguingly, the *socAB* operon is induced by the DNA-damaging agent MMC (Fig. 3A), suggesting that it may play a regulatory role during the response to DNA damage. One attractive possibility is that sublethal amounts of SocB accumulate following DNA damage, or other stresses, to regulate the rate at which replication proceeds. Recent work has begun to reveal mechanisms by which cells regulate replication at the level of elongation. For example, the accumulation of (p)ppGpp during the stringent response in *B. subtilis* leads to an arrest of replication elongation through the inhibition of DNA primase (Wang et al., 2007). Although replication is often controlled at the level of initiation, mechanisms for modulating elongation may be widespread.

Protein Interaction Hubs and Antibiotic Targets

In addition to blocking replication elongation, the binding of SocB to DnaN may disrupt other replication-associated processes. In addition to Pol III, the clamp interacts with proteins required for DNA repair and the regulation of replication initiation, including Pol IV and Pol V (translesion synthesis), MutS and MutL (mismatch repair), and Hda

NIH-PA Author Manuscript

NIH-PA Author Manuscript

NIH-PA Author Manuscript

(regulation of initiation). These proteins all bind to DnaN within the same hydrophobic cleft on its surface that is likely bound by SocB (Robinson et al., 2010), suggesting that SocB may disrupt several cellular processes required for growth and genome maintenance.

Interaction hubs such as DnaN may be ideal targets for new antibiotic development because they coordinate multiple cellular processes and may be unable to mutate to prevent small molecule binding without significantly compromising their native functions. The ability of a protein toxin like SocB to arrest DNA replication and kill cells suggests that the hydrophobic cleft on DnaN may be a prime target for small molecule inhibitors. In fact, the small molecule RU-7 was recently shown to bind within this hydrophobic cleft on the clamp and to prevent its association with Pol III *in vitro* (Georgescu et al., 2008). This interaction was specific for the bacterial sliding clamp, as the interaction between the eukaryotic PCNA clamp and Pol δ was unaffected. A separate screen for inhibitors of an *in vitro* bacterial replication system identified six compounds that share the same core structure as RU-7, suggesting that they also function through binding to the clamp (Dallmann et al., 2010). The recent rise in multi-drug resistant strains of various pathogenic bacteria highlights the continued need to develop novel antibiotics to combat these infections. The study of bacterially-encoded toxins and the mechanisms by which they inhibit cellular proliferation may prove valuable in the identification of promising new targets.

EXPERIMENTAL PROCEDURES

Bacterial Strains and Media

Caulobacter strains used in this study are listed in Table S1. For details on strain construction and growth conditions, see Extended Experimental Procedures.

Suppressor Screening and Mapping

Suppressors of a *clpP* depletion strain were obtained by EZ-Tn5 mutagenesis, and transposon insertion sites in surviving colonies were identified by rescue cloning of circularized DNA in *pir-116 E. coli*. Suppressors of *socB-M2* suppression were first screened for mutations in *socB*, *clpX*, and *clpP*; suppressors that contained no mutations in these genes were then subjected to whole genome sequencing to identify point mutations. For details, see Extended Experimental Procedures.

Protein Purification and Degradation Assays

His6-SocA and His6-SocB were purified by Ni-NTA affinity chromatography, and for His-SocA, by subsequent gel filtration chromatography (see Extended Experimental Procedures). ClpX, ΔN-ClpX, and ClpP were prepared as described previously (Chien et al., 2007). Degradation reactions were performed in PD-KCl-200 buffer at 4°C. Reaction conditions were as follows: 0.5 μM ClpX, 0.5 μM ΔN-ClpX, 1 μM ClpP, 5 μM SocB, 5 μM SocA, 32 μg/ml creatine kinase, 16 mM creatine phosphate, and 4 mM ATP.

Microscopy and Image Analysis

For details on image acquisition and processing, see Extended Experimental Procedures.

Microarrays

Expression data for cells exposed to the DNA-damaging agent mitomycin C was previously published (Modell et al., 2011). Expression profiling of cells expressing *socB-M2* was performed as described previously (Gora et al., 2010).

NIH-PA Author Manuscript

NIH-PA Author Manuscript

NIH-PA Author Manuscript

Supplementary Material

Refer to Web version on PubMed Central for supplementary material.

Acknowledgments

We thank members of the Laub laboratory for discussions and comments on the manuscript. We thank Peter Chien for providing purified ClpX, ΔN-ClpX, and ClpP. M.T.L. is an Early Career Investigator at the Howard Hughes Medical Institute. This work was supported by an HHMI Summer Medical Fellowship to D.H., an NSF Graduate Research Fellowship to C.D.A., and an NIH grant (R01GM082899) to M.T.L.

REFERENCES

Bhat NH, Vass RH, Stoddard PR, Shin DK, Chien P. Identification of ClpP substrates in *Caulobacter crescentus* reveals a role for regulated proteolysis in bacterial development. Mol. Microbiol. 2013; 88:1083–1092. [PubMed: 23647068]

Bunting KA, Roe SM, Pearl LH. Structural basis for recruitment of translesion DNA polymerase Pol IV/DinB to the beta-clamp. EMBO J. 2003; 22:5883–5892. [PubMed: 14592985]

Bush K, Courvalin P, Dantas G, Davies J, Eisenstein B, Huovinen P, Jacoby GA, Kishony R, Kreiswirth BN, Kutter E, et al. Tackling antibiotic resistance. Nat. Rev. Microbiol. 2011; 9:894–896. [PubMed: 22048738]

Castro-Roa D, Garcia-Pino A, De Geiter S, van Nuland NAJ, Loris R, Zenkin N. The Fic protein Doc uses an inverted substrate to phosphorylate and inactivate EF-Tu. Nat. Chem. Biol. 2013 in press.

Chien P, Perchuk BS, Laub MT, Sauer RT, Baker TA. Direct and adaptor-mediated substrate recognition by an essential AAA+ protease. Proc. Natl. Acad. Sci. USA. 2007; 104:6590–6595. [PubMed: 17420450]

Christen B, Abeliuk E, Collier JM, Kalogeraki VS, Passarelli B, Coller JA, Fero MJ, McAdams HH, Shapiro L. The essential genome of a bacterium. Mol. Syst. Biol. 2011; 7:528. [PubMed: 21878915]

Coates AR, Halls G, Hu Y. Novel classes of antibiotics or more of the same? Br. J. Pharmacol. 2011; 163:184–194. [PubMed: 21323894]

Collier J, Shapiro L. Feedback control of DnaA-mediated replication initiation by replisome-associated HdaA protein in *Caulobacter*. J. Bacteriol. 2009; 191:5706–5716. [PubMed: 19633089]

Dallmann HG, Fackelmayer OJ, Tomer G, Chen J, Wiktor-Becker A, Ferrara T, Pope C, Oliveira MT, Burgers PM, Kaguni LS, et al. Parallel multiplicative target screening against divergent bacterial replicases: identification of specific inhibitors with broad spectrum potential. Biochemistry. 2010; 49:2551–2562. [PubMed: 20184361]

Dalrymple BP, Kongsuwan K, Wijffels G, Dixon NE, Jennings PA. A universal protein-protein interaction motif in the eubacterial DNA replication and repair systems. Proc. Natl. Acad. Sci. USA. 2001; 98:11627–11632. [PubMed: 11573000]

Dougan DA, Weber-Ban E, Bukau B. Targeted delivery of an ssrA-tagged substrate by the adaptor protein SspB to its cognate AAA+ protein ClpX. Mol. Cell. 2003; 12:373–380. [PubMed: 14536077]

Farrell CM, Baker TA, Sauer RT. Altered specificity of a AAA+ protease. Mol. Cell. 2007; 25:161–166. [PubMed: 17218279]

Flynn JM, Neher SB, Kim YI, Sauer RT, Baker TA. Proteomic discovery of cellular substrates of the ClpXP protease reveals five classes of ClpX-recognition signals. Mol. Cell. 2003; 11:671–683. [PubMed: 12667450]

Georgescu RE, Yurieva O, Kim SS, Kuriyan J, Kong XP, O'Donnell M. Structure of a small-molecule inhibitor of a DNA polymerase sliding clamp. Proc. Natl. Acad. Sci. USA. 2008; 105:11116–11121. [PubMed: 18678908]

Gerdes K, Maisonneuve E. Bacterial persistence and toxin-antitoxin loci. Annu. Rev. Microbiol. 2012; 66:103–123. [PubMed: 22994490]

Gora KG, Tsokos CG, Chen YE, Srinivasan BS, Perchuk BS, Laub MT. A cell-type-specific protein-protein interaction modulates transcriptional activity of a master regulator in *Caulobacter crescentus*. Mol. Cell. 2010; 39:455–467. [PubMed: 20598601]

NIH-PA Author Manuscript NIH-PA Author Manuscript NIH-PA Author Manuscript

Indiani C, McInerney P, Georgescu R, Goodman MF, O'Donnell M. A sliding-clamp toolbelt binds high- and low-fidelity DNA polymerases simultaneously. Mol. Cell. 2005; 19:805–815. [PubMed: 16168375]

Jenal U, Fuchs T. An essential protease involved in bacterial cell-cycle control. EMBO J. 1998; 17:5658–5669. [PubMed: 9755166]

Johnson A, O'Donnell M. Cellular DNA replicases: components and dynamics at the replication fork. Annu. Rev. Biochem. 2005; 74:283–315. [PubMed: 15952889]

Jonas K, Chen YE, Laub MT. Modularity of the bacterial cell cycle enables independent spatial and temporal control of DNA replication. Curr. Biol. 2011; 21:1092–1101. [PubMed: 21683595]

Karimova G, Pidoux J, Ullmann A, Ladant D. A bacterial two-hybrid system based on a reconstituted signal transduction pathway. Proc. Natl. Acad. Sci. USA. 1998; 95:5752–5756. [PubMed: 9576956]

Kato J, Katayama T. Hda, a novel DnaA-related protein, regulates the replication cycle in *Escherichia coli*. EMBO J. 2001; 20:4253–4262. [PubMed: 11483528]

Kurz M, Dalrymple B, Wijffels G, Kongsuwan K. Interaction of the sliding clamp beta-subunit and Hda, a DnaA-related protein. J. Bacteriol. 2004; 186:3508–3515. [PubMed: 15150238]

Lenhart JS, Sharma A, Hingorani MM, Simmons LA. DnaN clamp zones provide a platform for spatiotemporal coupling of mismatch detection to DNA replication. Mol. Microbiol. 2013; 87:553–568. [PubMed: 23228104]

Lenne-Samuel N, Wagner J, Etienne H, Fuchs RP. The processivity factor beta controls DNA polymerase IV traffic during spontaneous mutagenesis and translesion synthesis in vivo. EMBO Rep. 2002; 3:45–49. [PubMed: 11751576]

Levchenko I, Seidel M, Sauer RT, Baker TA. A specificity-enhancing factor for the ClpXP degradation machine. Science. 2000; 289:2354–2356. [PubMed: 11009422]

Little JW, Mount DW. The SOS regulatory system of *Escherichia coli* . Cell. 1982; 29:11–22. [PubMed: 7049397]

Lopez de Saro FJ, Marinus MG, Modrich P, O'Donnell M. The beta sliding clamp binds to multiple sites within MutL and MutS. J. Biol. Chem. 2006; 281:14340–14349. [PubMed: 16546997]

Maki S, Kornberg A. DNA polymerase III holoenzyme of *Escherichia coli* II. A novel complex including the gamma subunit essential for processive synthesis. J. Biol. Chem. 1988; 263:6555–6560. [PubMed: 3283126]

Martin A, Baker TA, Sauer RT. Diverse pore loops of the AAA+ ClpX machine mediate unassisted and adaptor-dependent recognition of ssrA-tagged substrates. Mol. Cell. 2008; 29:441–450. [PubMed: 18313382]

Modell JW, Hopkins AC, Laub MT. A DNA damage checkpoint in *Caulobacter crescentus* inhibits cell division through a direct interaction with FtsW. Genes Dev. 2011; 25:1328–1343. [PubMed: 21685367]

Mutschler H, Gebhardt M, Shoeman RL, Meinhart A. A novel mechanism of programmed cell death in bacteria by toxin-antitoxin systems corrupts peptidoglycan synthesis. PLoS Biol. 2011; 9:e1001033. [PubMed: 21445328]

Nakano MM, Hajarizadeh F, Zhu Y, Zuber P. Loss-of-function mutations in yjbD result in ClpX- and ClpP-independent competence development of Bacillus subtilis. Mol. Microbiol. 2001; 42:383–394. [PubMed: 11703662]

Pandey DP, Gerdes K. Toxin-antitoxin loci are highly abundant in free-living but lost from host-associated prokaryotes. Nucleic Acids Res. 2005; 33:966–976. [PubMed: 15718296]

Piotrowski A, Burghout P, Morrison DA. spr1630 is responsible for the lethality of clpX mutations in *Streptococcus pneumoniae*. J. Bacteriol. 2009; 191:4888–4895. [PubMed: 19465654]

Raju RM, Unnikrishnan M, Rubin DH, Krishnamoorthy V, Kandror O, Akopian TN, Goldberg AL, Rubin EJ. *Mycobacterium tuberculosis* ClpP1 and ClpP2 function together in protein degradation and are required for viability in vitro and during infection. PLoS Pathog. 2012; 8:e1002511. [PubMed: 22359499]

Robinson A, Brzoska AJ, Turner KM, Withers R, Harry EJ, Lewis PJ, Dixon NE. Essential biological processes of an emerging pathogen: DNA replication, transcription, and cell division in *Acinetobacter* spp. Microbiol. Mol. Biol. Rev. 2010; 74:273–297. [PubMed: 20508250]

NIH-PA Author Manuscript

NIH-PA Author Manuscript

NIH-PA Author Manuscript

Robinson A, Causer RJ, Dixon NE. Architecture and conservation of the bacterial DNA replication machinery, an underexploited drug target. Curr. Drug Targets. 2012; 13:352–372. [PubMed: 22206257]

Sauer RT, Baker TA. AAA+ proteases: ATP-fueled machines of protein destruction. Annu. Rev. Biochem. 2011; 80:587–612. [PubMed: 21469952]

Schweder T, Lee KH, Lomovskaya O, Matin A. Regulation of *Escherichia coli* starvation sigma factor (sigma s) by ClpXP protease. J. Bacteriol. 1996; 178:470–476. [PubMed: 8550468]

Su'etsugu M, Errington J. The replicase sliding clamp dynamically accumulates behind progressing replication forks in *Bacillus subtilis* cells. Mol. Cell. 2011; 41:720–732. [PubMed: 21419346]

Walsh, C. Antibiotics: actions, origins, resistance. Washington, D.C.: ASM Press; 2003.

Wang JD, Sanders GM, Grossman AD. Nutritional control of elongation of DNA replication by (p)ppGpp. Cell. 2007; 128:865–875. [PubMed: 17350574]

Wang X, Kim Y, Hong SH, Ma Q, Brown BL, Pu M, Tarone AM, Benedik MJ, Peti W, Page R, et al. Antitoxin MqsA helps mediate the bacterial general stress response. Nat. Chem. Biol. 2011; 7:359–366. [PubMed: 21516113]

Yamaguchi Y, Inouye M. Regulation of growth and death in *Escherichia coli* by toxin-antitoxin systems. Nat. Rev. Microbiol. 2011; 9:779–790. [PubMed: 21927020]

Yamaguchi Y, Park JH, Inouye M. Toxin-antitoxin systems in bacteria and archaea. Annu. Rev. Genet. 2011; 45:61–79. [PubMed: 22060041]

Yuan J, Sterckx Y, Mitchenall LA, Maxwell A, Loris R, Waldor MK. *Vibrio cholerae* ParE2 poisons DNA gyrase via a mechanism distinct from other gyrase inhibitors. J. Biol. Chem. 2010; 285:40397–40408. [PubMed: 20952390]

Zhang Y, Zhang J, Hoeflich KP, Ikura M, Qing G, Inouye M. MazF cleaves cellular mRNAs specifically at ACA to block protein synthesis in *Escherichia coli*. Mol. Cell. 2003; 12:913–923. [PubMed: 14580342]

NIH-PA Author Manuscript

NIH-PA Author Manuscript

NIH-PA Author Manuscript

HIGHLIGHTS

- SocAB is an atypical toxin-antitoxin system in *Caulobacter crescentus*
- The antitoxin SocA is required for ClpXP-mediated degradation of the toxin SocB
- In the absence of SocA or ClpXP, SocB accumulates and inhibits DNA replication
- SocB inhibits replication by binding the β sliding clamp

NIH-PA Author Manuscript
NIH-PA Author Manuscript
NIH-PA Author Manuscript

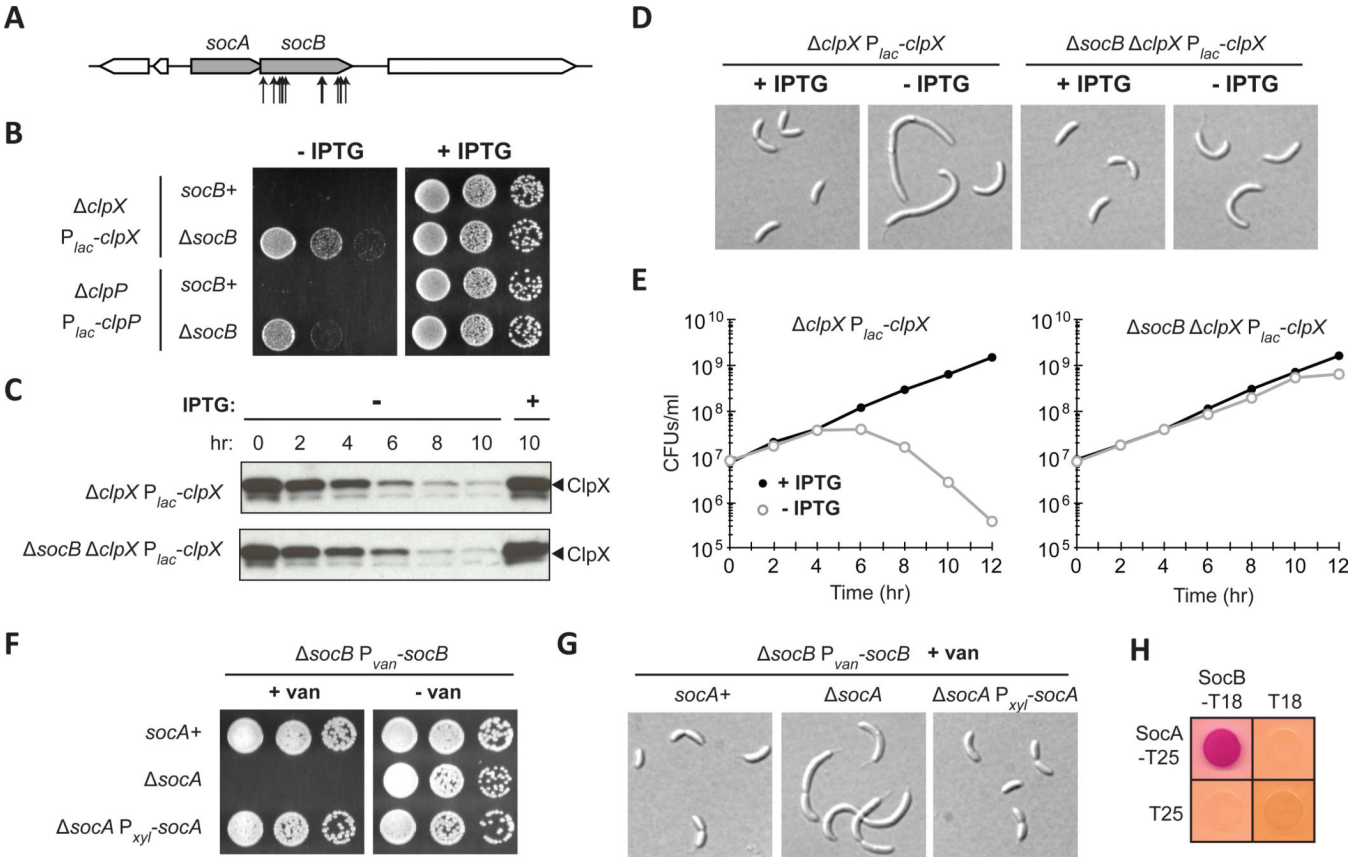

Fig. 1. Mutations in the Toxin *socB* Bypass ClpXP Essentiality

(A) Schematic of transposon insertions in *socB* (CCNA_03629) that suppressed the essentiality of *clpP*.

(B) Growth of *clpX* and *clpP* depletion strains in *socB*+ and Δ*socB* backgrounds. Five-fold serial dilutions of the indicated strains were spotted onto media ± IPTG.

(C) Kinetics of ClpX depletion. Indicated strains were shifted to media ± IPTG, and samples were subjected to immunoblotting.

(D) Morphology of cells following ClpX depletion in *socB*+ and Δ*socB* backgrounds. Strains from (C) were imaged by DIC microscopy at 10 hr.

(E) Viability of cells following ClpX depletion in *socB*+ and Δ*socB* backgrounds. Colony forming units (CFUs)/ml of the strains from (C) are shown; mean of two biological replicates.

(F) Growth of strains expressing *socB* in the *socA*+ or Δ*socA* backgrounds. The indicated strains were five-fold serially diluted onto media that induces or represses *socB*.

(G) Morphology of strains from (F). The indicated strains were grown for 4 hr in *socB* inducing conditions and then imaged by DIC microscopy.

(H) Bacterial two-hybrid analysis of the interaction between SocA and SocB. T18/T25 were included as a negative control; red indicates a positive interaction. Cells were grown for 1 day at 30°C.

See also Fig. S1.

NIH-PA Author Manuscript

NIH-PA Author Manuscript

NIH-PA Author Manuscript

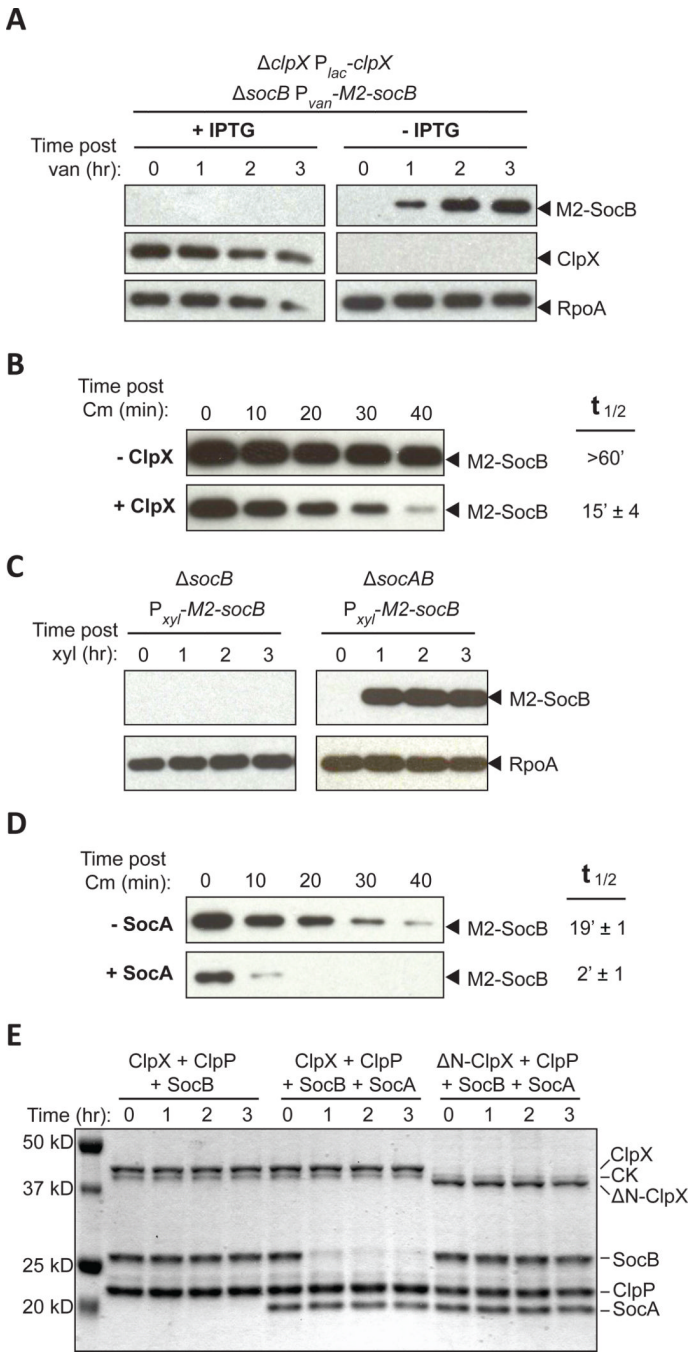

Fig. 2. SocA Promotes SocB Degradation by ClpXP

(A) Abundance of M2-SocB ± ClpX assessed by immunoblotting. The indicated strain was grown in *clpX* inducing or repressing conditions for 12 hr and *M2-socB* expression was induced at time zero. RpoA is a loading control.

(B) Stability of M2-SocB ± ClpX. *clpX* expression was repressed or induced for 12 hr, and then *M2-socB* expression was induced for 30 min prior to chloramphenicol (Cm) addition at time zero to shut off protein synthesis. Half-life ± S.E.M. quantified from three replicates (see Fig. S2A).

(C) Abundance of M2-SocB ± SocA assessed by immunoblotting. *M2-socB* expression was induced at time zero.

NIH-PA Author Manuscript

NIH-PA Author Manuscript

NIH-PA Author Manuscript

(D) Stability of M2-SocB ± SocA. *M2-socB* expression was induced for 2 hr, and then *socA* expression was induced for an additional 40 min prior to Cm addition at time zero. Half-life ± S.E.M. quantified from three replicates (see Fig. S2B).
(E) *In vitro* degradation of SocB by ClpXP ± SocA. Amounts were: 0.5 μM ClpX or ΔN-ClpX, 1 μM ClpP, 5 μM SocB, 5 μM SocA, 32 μg/ml creatine kinase (CK), 16 mM creatine phosphate, and 4 mM ATP. Reaction performed at 4°C.
See also Fig. S2.

NIH-PA Author Manuscript
NIH-PA Author Manuscript
NIH-PA Author Manuscript

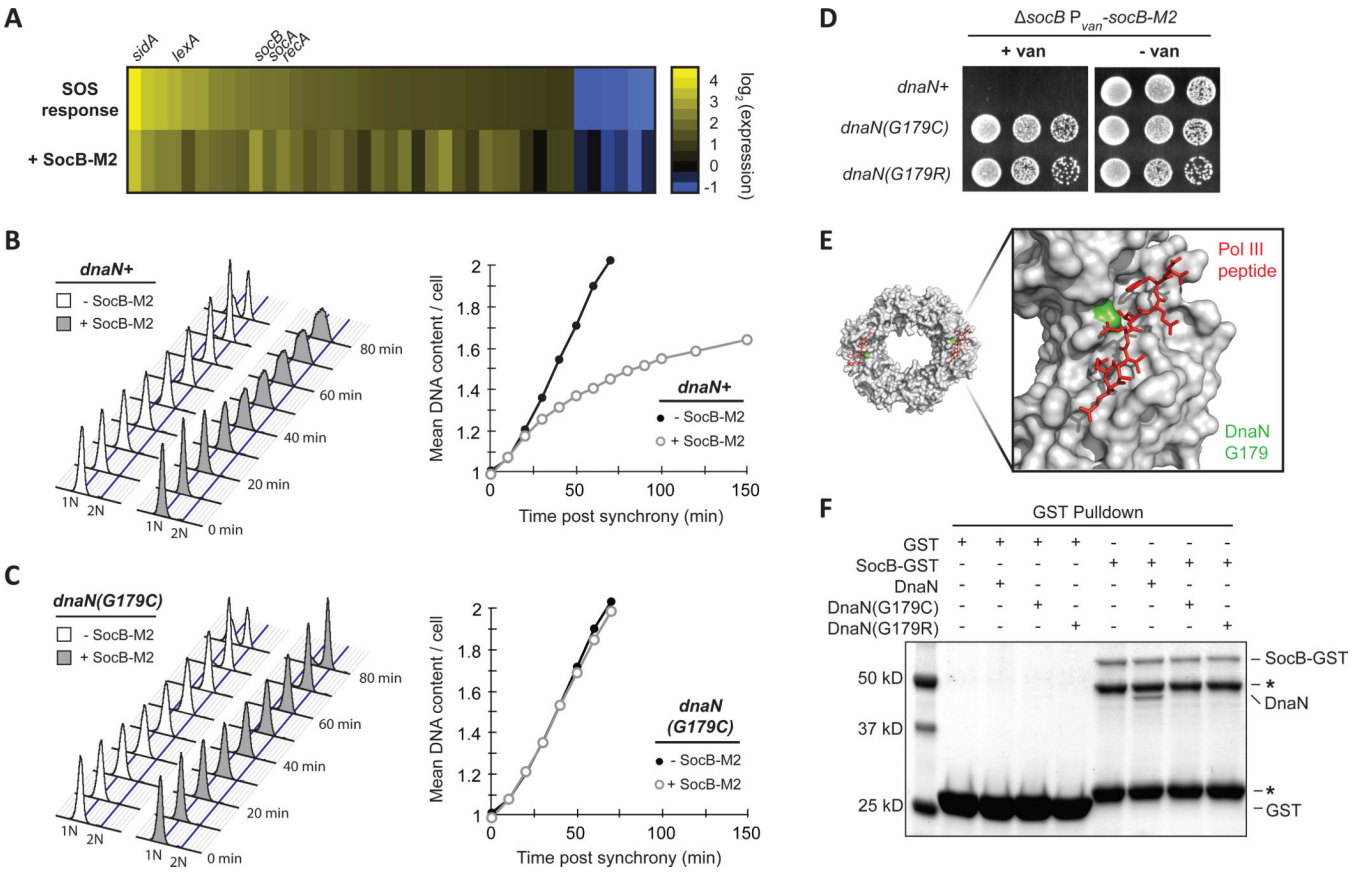

Fig. 3. SocB Blocks Replication Elongation Through an Interaction with DnaN

(A) Analysis of gene expression changes following exposure to the DNA-damaging agent mitomycin C for 30 min (SOS response, top row) or following *socB-M2* expression for 2 hr (+SocB-M2, bottom row). For each treatment, the genes induced or repressed more than 2-fold following mitomycin C treatment are shown.

(B) Flow cytometry of DNA content from synchronized cells grown ± *socB-M2* expression. For the +SocB-M2 condition, *socB-M2* was induced for 90 min prior to synchrony and release. Quantification of DNA content is shown on right.

(C) Same as (B), except performed with the *dnaN(G179C)* strain.

(D) Growth of indicated strains on *socB-M2* inducing or repressing medium. Five-fold serial dilutions are shown.

(E) Structure of the *E. coli* sliding clamp in complex with a peptide derived from Pol III (PDB: 3D1F). Pol III peptide is in red, and the *E. coli* residue that corresponds to G179 in *Caulobacter* is colored in green.

(F) Interaction between SocB-GST and DnaN. For each condition, the indicated proteins were mixed with glutathione sepharose beads, washed, eluted, and then loaded on an SDS-PAGE gel. SocB-GST protein is unstable; asterisks indicate truncated SocB-GST products that retain GST tag.

See also Fig. S3.

NIH-PA Author Manuscript
NIH-PA Author Manuscript
NIH-PA Author Manuscript

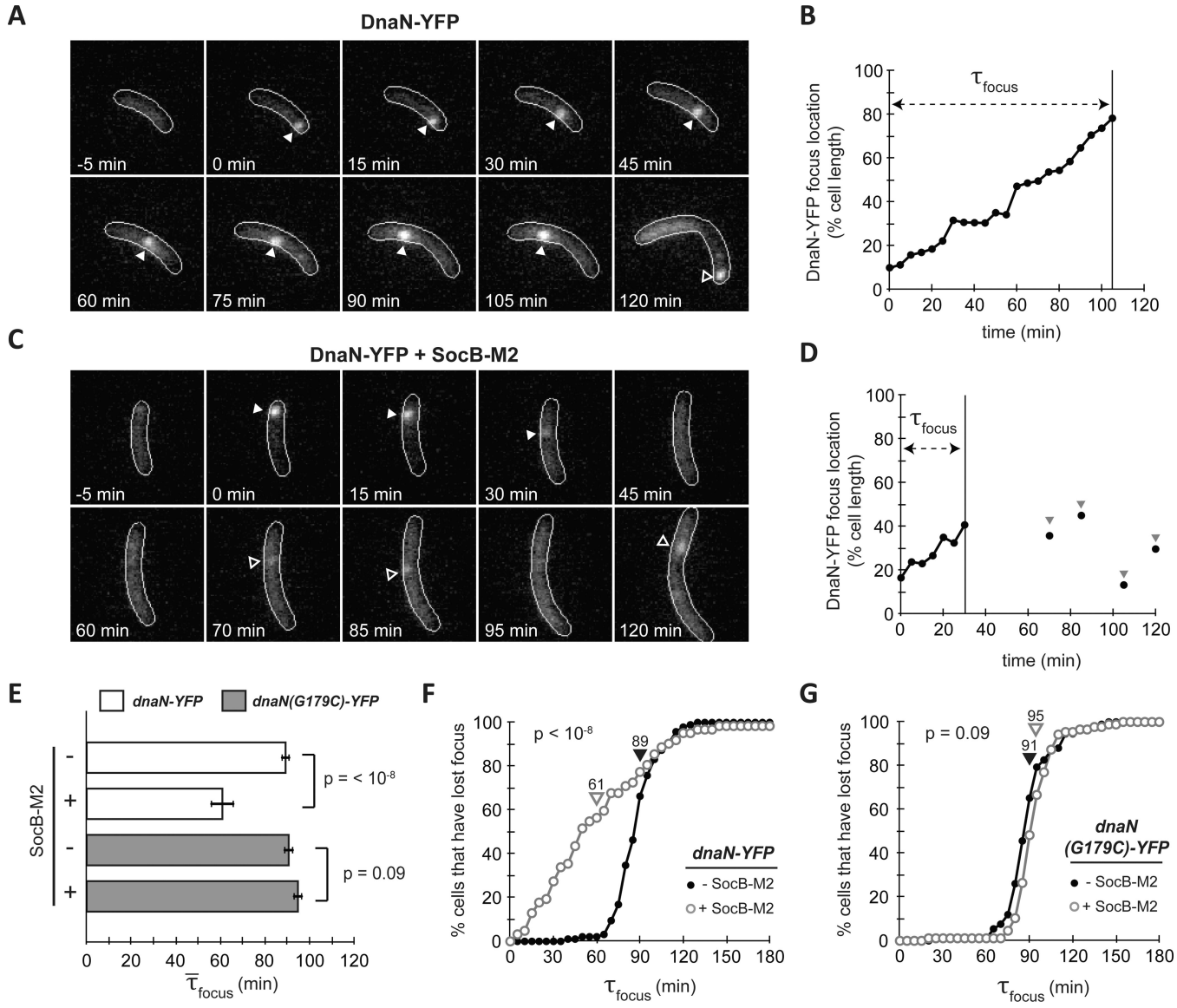

Fig. 4. SocB Induces Replication Fork Collapse

(A) Fluorescence microscopy of strain bearing *dnaN-YFP* on a low-copy plasmid. *dnaN-YFP* was pre-induced for 2 h, and cells were synchronized and imaged every 5 min. Filled arrows indicates calculated position of DnaN-YFP focus; hollow arrows indicate a new round of replication following division.

(B) Calculated DnaN-YFP focus position of the cell from (A). τ_{focus} is calculated as the time from focus formation to loss.

(C–D) Same as (A–B), except *socB-M2* expression was induced for 90 min prior to synchrony and following release. Note the pre-mature focus loss between 30 and 45 min. Hollow arrows indicate transient DnaN-YFP focus formation events that may be attempts at replication restart.

(E) Average τ_{focus} for *dnaN-YFP* strain (white bars) and *dnaN(G179C)-YFP* strain (grey bars) ± *socB-M2* expression. Error bars indicate ± S.E.M; n≥60 cells per condition.

(F) Percentage of cells that have lost their DnaN-YFP focus as a function of time post initiation in the absence (filled circles) or presence (hollow circles) of *socB-M2* expression. Average τ_{focus} denoted by arrows. n≥60 cells per condition.

(G) Same as (F), but with *dnaN(G179C)-YFP* strain. n≥60 cells per condition.

NIH-PA Author Manuscript

NIH-PA Author Manuscript

NIH-PA Author Manuscript

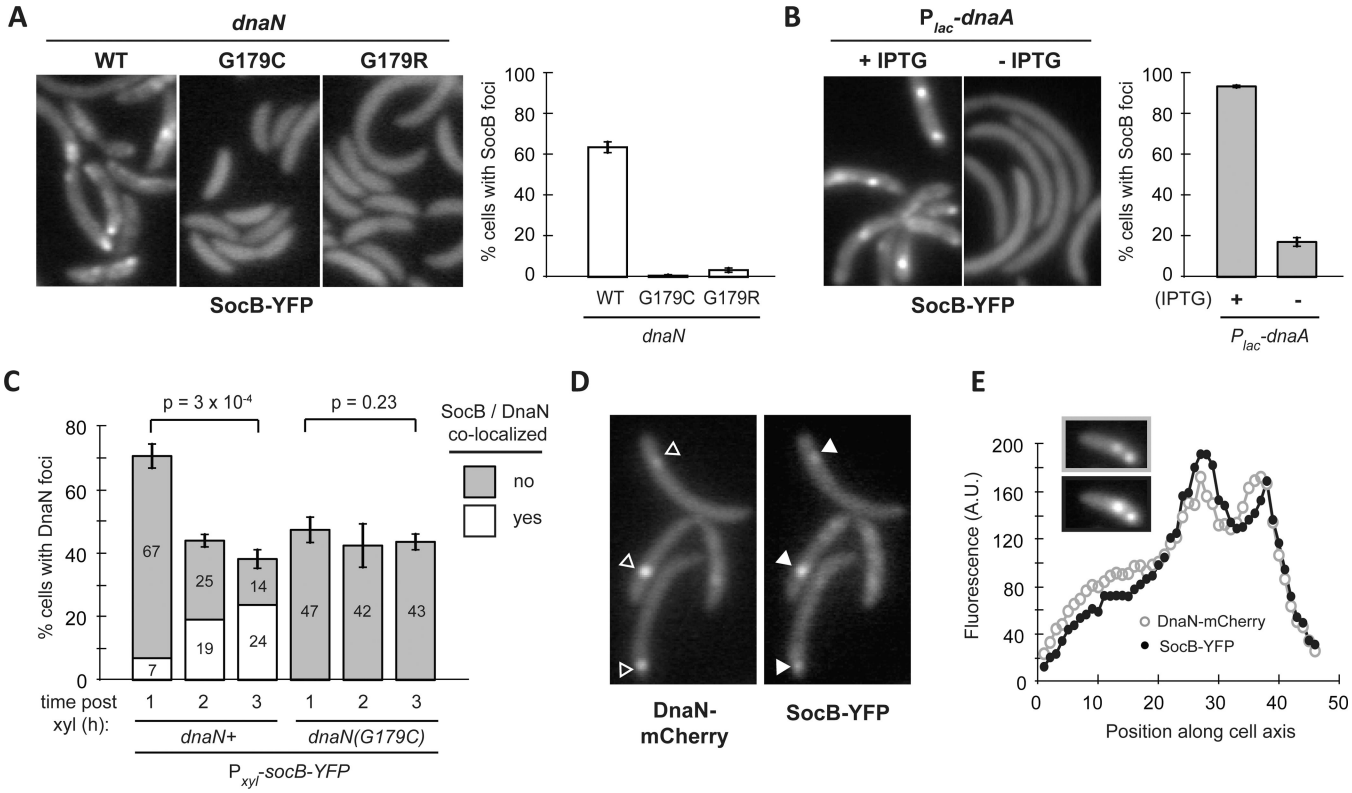

Fig. 5. SocB Forms Foci that Co-Localize with DnaN

(A) Fluorescence microscopy of indicated strains at 3 hr post *socB-YFP* induction. Percentage of cells containing SocB-YFP foci is shown on the right. Errors bars indicate mean ± S.D. for three biological replicates (n>400 cells per replicate).

(B) Fluorescence microscopy of P_{lac}-*dnaA* cells grown in the presence or absence of IPTG for 2 hr prior to *socB-YFP* induction for 3 h. Percentage of cells containing SocB-YFP foci calculated as in (A). Errors bars indicate mean ± S.D. for three biological replicates (n>400 cells per replicate).

(C) Percentage of cells with DnaN-mCherry foci as a function of time post *socB-YFP* induction. The percentage of total cells with co-localized (white) or not co-localized (grey) DnaN-mCherry and SocB-YFP foci is shown within each bar. Error bars indicate mean ± S.D. for three biological replicates (n>500 cells per replicate).

(D) Co-localization of DnaN-mCherry foci (hollow arrows) and SocB-YFP foci (filled arrows) after induction of *socB-YFP* for 3 h.

(E) Co-localization of multiple DnaN-mCherry and SocB-YFP foci in a single cell. Fluorescence profile for DnaN-mCherry (top inset, grey hollow circles) and SocB-YFP (bottom inset, black filled circles) is shown.

See also Fig. S4.

NIH-PA Author Manuscript NIH-PA Author Manuscript NIH-PA Author Manuscript

NIH-PA Author Manuscript

NIH-PA Author Manuscript

NIH-PA Author Manuscript

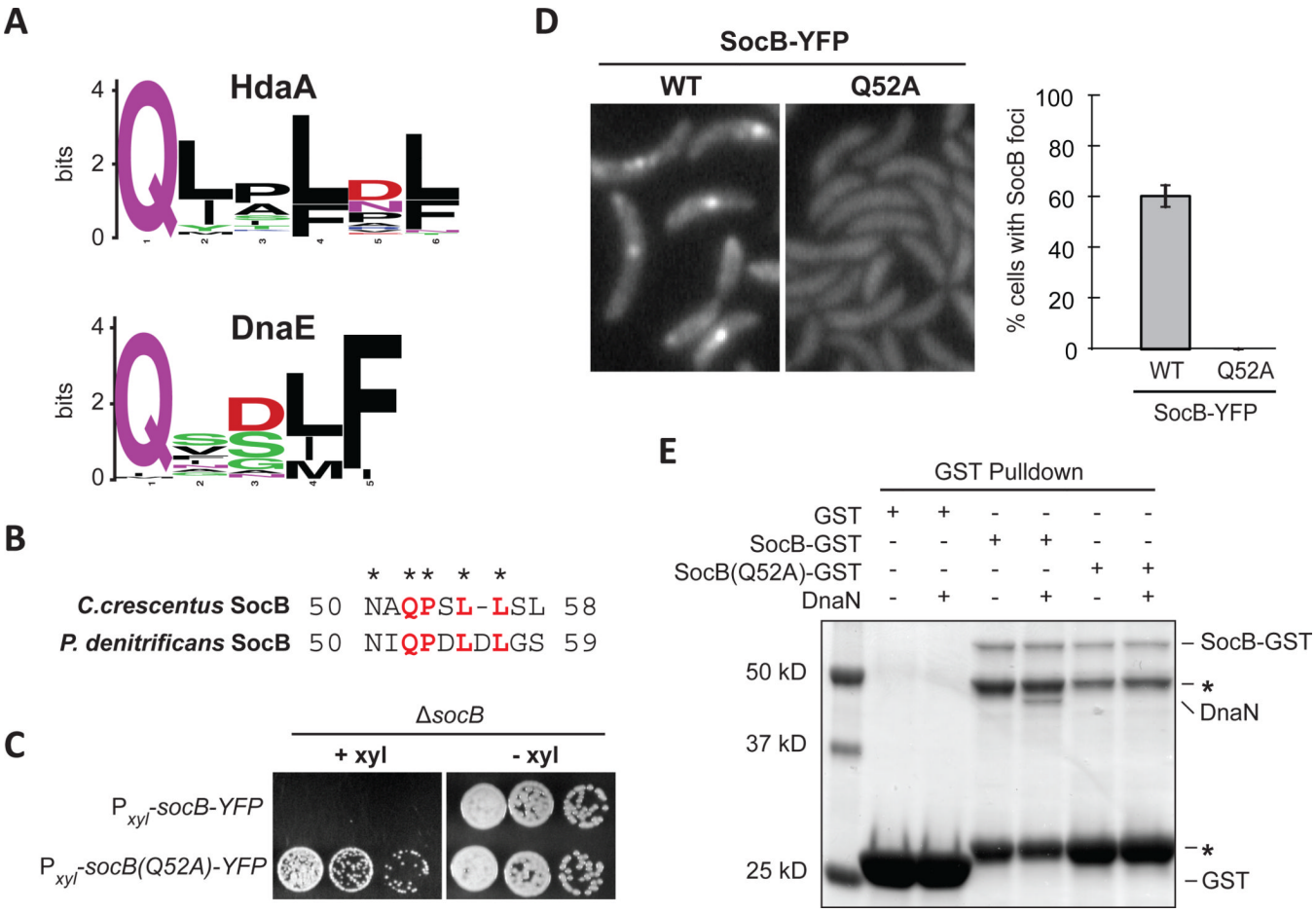

Fig. 6. SocB Interacts with DnaN Through a Conserved Motif

(A) Sequence logo of the DnaN-binding motif in HdaA or DnaE from α-proteobacteria.

(B) Putative DnaN-binding motif in SocB from *C. crescentus* and *P. denitrificans*.

(C) Growth of indicated strains on media that induces (+xyl) or represses (−xyl) *socB-YFP* or *socB(Q52A)-YFP* expression. Five-fold serial dilutions are shown.

(D) Fluorescence microscopy of *socB-YFP* or *socB(Q52A)-YFP* 3 hr post induction. Percentage of cells with SocB-YFP foci ± S.D. for three biological replicates is shown on right (n>500 cells per replicate).

(E) Interaction between SocB-GST, SocB(Q52A)-GST, and DnaN. Performed as in Fig. 3H; as before, asterisk indicates SocB-GST N-terminal degradation products.

See also Fig. S5.

NIH-PA Author Manuscript

NIH-PA Author Manuscript

NIH-PA Author Manuscript

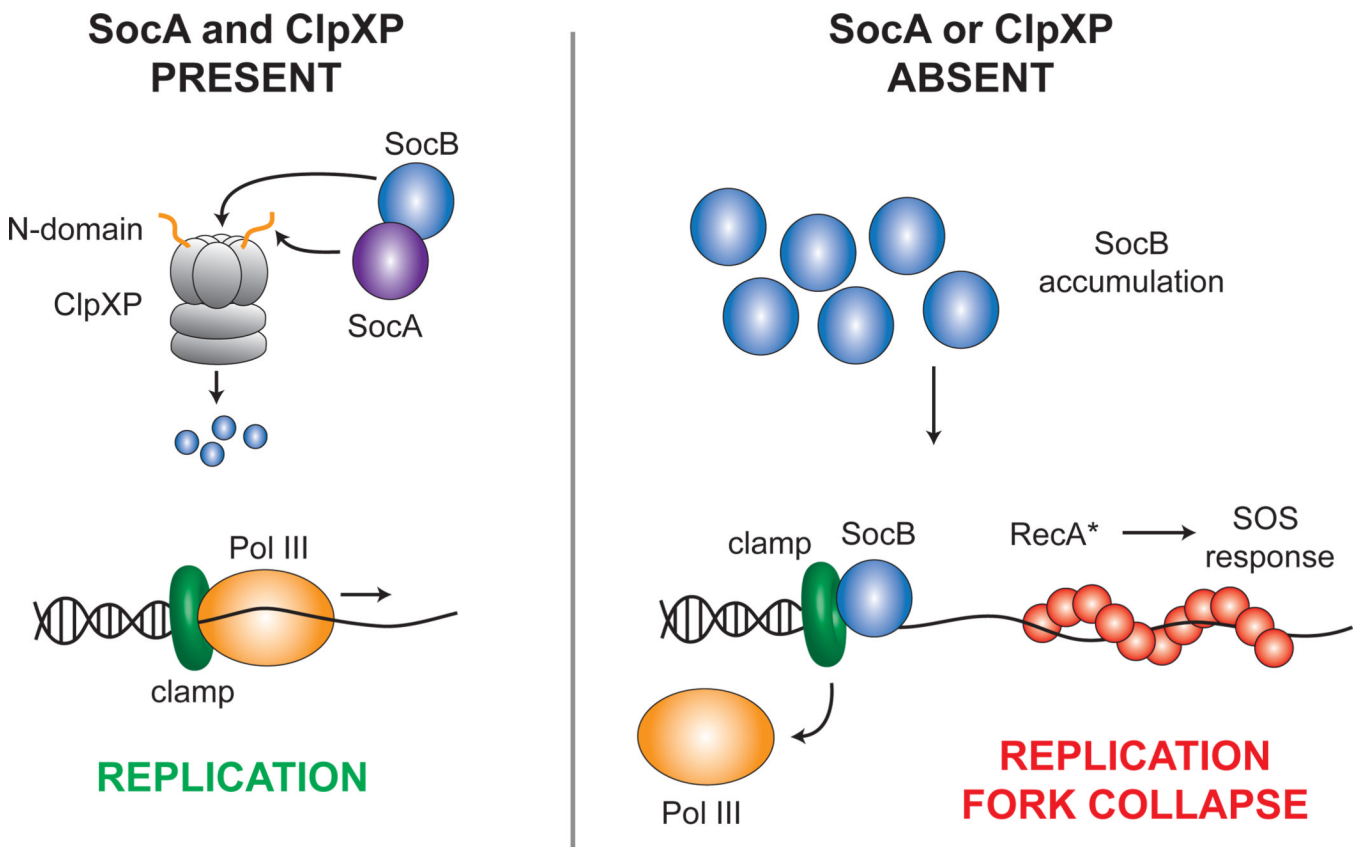

Fig. 7. Model for SocAB Function

Under normal growth conditions, the toxin SocB is delivered to ClpXP for degradation by its antitoxin SocA. Pol III thus remains in association with the clamp, and replication proceeds normally (left). However, in the absence of either ClpXP or SocA, SocB accumulates and competes for binding to the clamp with Pol III and other replication factors. This competition eventually results in the collapse of replication forks and induction of the RecA-mediated SOS response (right).